



**HAL**  
open science

# Route to chaos in a circuit modeled by a 1-dimensional piecewise linear map

Danièle Fournier-Prunaret, Pascal Charge

► **To cite this version:**

Danièle Fournier-Prunaret, Pascal Charge. Route to chaos in a circuit modeled by a 1-dimensional piecewise linear map. *Nonlinear Theory and Its Applications, IEICE*, 2012, 3 (4), pp.521-532. 10.1587/nolta.3.521 . hal-00707750

**HAL Id: hal-00707750**

**<https://hal.science/hal-00707750>**

Submitted on 8 Oct 2020

**HAL** is a multi-disciplinary open access archive for the deposit and dissemination of scientific research documents, whether they are published or not. The documents may come from teaching and research institutions in France or abroad, or from public or private research centers.

L'archive ouverte pluridisciplinaire **HAL**, est destinée au dépôt et à la diffusion de documents scientifiques de niveau recherche, publiés ou non, émanant des établissements d'enseignement et de recherche français ou étrangers, des laboratoires publics ou privés.



Distributed under a Creative Commons Attribution 4.0 International License

# Route to chaos in a circuit modeled by a 1-dimensional piecewise linear map

*Danièle Fournier-Prunaret<sup>1a)</sup> and Pascal Chargé<sup>2b)</sup>*

<sup>1</sup> *INSA, Université de Toulouse*

*LAAS-CNRS, 7 avenue du colonel Roche, F-31077 Toulouse Cedex 4, France*

<sup>2</sup> *Lunam University, University of Nantes*

*UMR CNRS 6164 IETR, Polytech Nantes, France*

<sup>a)</sup> *daniele.fournier@insa-toulouse.fr*

<sup>b)</sup> *pascal.charge@univ-nantes.fr*

**Abstract:** A very simple hybrid circuit proposed as chaos generator is studied. It is modeled using a 3-slopes piecewise linear map defined on  $[0,1]$  and depending upon three parameters. The parameter space is investigated in order to classify regions of existence of stable periodic orbits and regions associated with chaotic behaviors. Bifurcation curves are obtained numerically and analytically. Border collision bifurcations and homoclinic bifurcations occurring in cyclical chaotic regions leading to chaos in one-piece are detected.

**Key Words:** piecewise linear bimodal map, chaos generator, border collision bifurcation

## 1. Introduction

Many circuits including switches have been considered during the last decade. Such systems are of interest for two reasons: first, they belong to the class of hybrid systems that have attracted much interest those last ten years, secondly, they permit to obtain chaos in a very easy way. Hybrid systems have been much considered in many kinds of applications during the last decade. Such systems appear for example in Electronics and Electrotechnics and the understanding of their behaviour is of great interest. Hybrid systems evolve in continuous time, but it is possible to model them using discrete time maps, by introducing a discretization similar to the building of a Poincaré map. This is the case for the circuit we consider in this paper. Concerning the second point, chaotic signals have appeared as very useful in many kinds of applications in the last twenty years, particularly in telecommunications and image processing. Indeed, for some kind of applications, it is necessary to consider robust chaos [1], which can endure, even if parameter values are slightly modified. A way to obtain robust chaotic signals is to consider systems where border collision bifurcations appear [2, 3, 6, 8, 9], that generally constitute a class of hybrid systems. Chaotic generators can also be obtained using continuous time models as systems based on the Chua's circuit (analogical circuit), while others are discrete time systems which directly iterate a chaotic map (digital circuit). The problem with these systems is that chaos is not necessarily as robust.

In this paper, we propose a chaos generator obtained from a simple RC circuit including switches

managed using a clock (impulse waveform) and the charging/discharging of the capacitor. We have previously proposed such a kind of chaos generator, where the model was a two-dimensional nonlinear map [4, 5, 10]. Our aim in considering a one-dimensional case is to analyze rigorously the bifurcations and to prove the existence of chaos in an even more simple circuit.

The section 2 is devoted to the description of the circuit and its modeling. The model under a one-dimensional piecewise linear map is given in section 3. The dynamical behaviour of the map, with the study of bifurcations permitting to obtain periodic orbits and chaos is explained for some parameter values in section 4.

## 2. Description of the circuit

The 1D proposed chaos generator is a quite simple circuit given in Fig. 1, very similar to those discussed in [3, 6]. The analog state variable is  $V(t)$ , the voltage across the capacitor. We can see that the switch position is ruled by the logic subsystem output  $p$ . In the same time inputs of the logic subsystem are provided by comparison of the analog state variable  $V(t)$  with constant voltages  $V_U$  and  $V_D$ . Analog and logic subsystems then form a hybrid system.

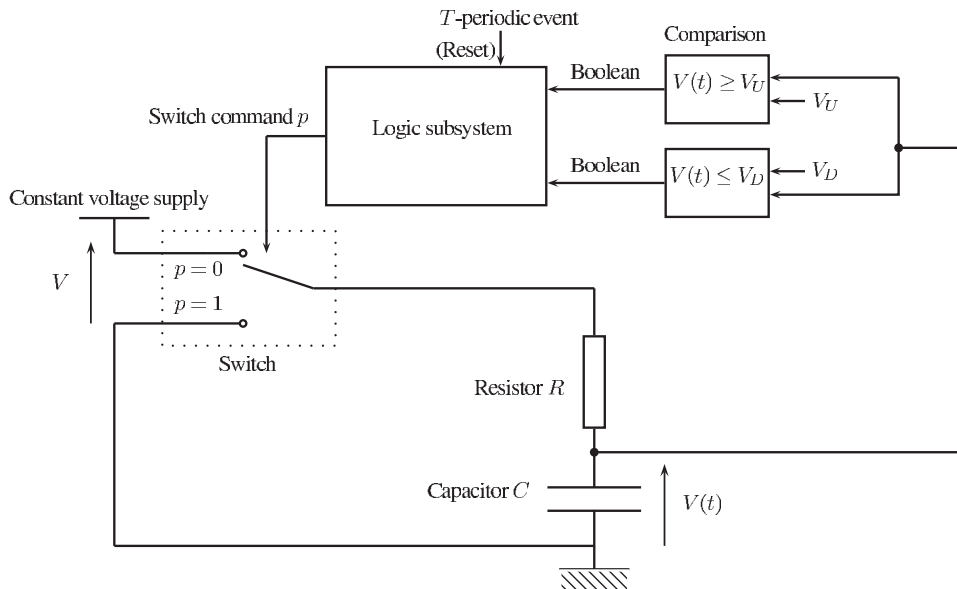


**Fig. 1.** The hybrid circuit including the analog and logic subsystems.

Behavior of the logic subsystem can be described by the following finite state diagram. At any state transition, the condition is given by the boolean expression above the line, whereas the action at the transition is indicated below the same line. As an example, the transition from the state  $C_1$  to the state  $D$  occurs when the expression  $((t < T) \& (V(t) \geq V_U))$  is true. At this transition instant, the system output  $p$  is set to the logic value 1. Actions are then described with variables allocations. The variable  $t$  denotes the time. When the time reaches the value  $t = T$ , a state transition is expected and the time variable is reset (allocation  $t := 0$ ).

From this diagram observation, it comes that the logic subsystem is an asynchronous sequential system, that is periodically forced to return to the state  $C_1$  by an external periodic event. In [11, 15], we proposed a very simple implementation of this logic subsystem based on a few R-S latches and logic operators. The periodic event is then realized thanks to a pulse generator.

A switch occurs at every  $T$ -periodic event or when the state variable  $V(t)$  reaches the value of  $V_D$  or  $V_U$ . The capacitor charges ( $p=0$ ) when  $V(t)$  reaches  $V_D$  or discharges ( $p=1$ ) when  $V(t)$  reaches  $V_U$ . Let us call  $V$  the reference voltage,  $V_A$  the borderline value corresponding to  $V(t) = V_U$ ,  $V_B$  the borderline value corresponding to  $V(t) = V_D$  and  $\tau = RC$ . Let us call  $V$  the reference voltage, namely the constant voltage supply in the circuit. Then, we can propose a model for our system.

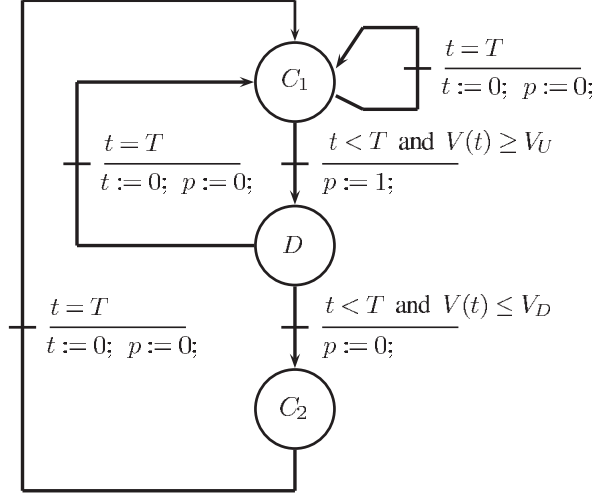


**Fig. 2.** The finite state diagram, which describes the logic subsystem.

### 3. Modeling

By considering the classical equations of a RC circuit, we obtain  $V_A = V - (V - V_U)e^{\frac{T}{\tau}}$ ,  $V_B = V - \frac{V_D}{V_U}(V - V_U)e^{\frac{T}{\tau}}$ . Let us call  $V_n$ , the state value at each time  $t = T$  when the time is initialized again, we obtain the following relations:

$$\begin{aligned}
 0 < V_n \leq V_A \quad , \quad V_{n+1} &= V - (V - V_n)e^{-\frac{T}{\tau}} \\
 V_A < V_n < V_B \quad , \quad V_{n+1} &= (V - V_n)\frac{V_U}{V - V_U}e^{-\frac{T}{\tau}} \\
 V_B < V_n \leq 1 \quad , \quad V_{n+1} &= V - (V - V_n)\frac{V_U}{V_D}\frac{V - V_D}{V - V_U}e^{-\frac{T}{\tau}}
 \end{aligned} \tag{1}$$

We normalize the state variables and the parameters in order to deal with dimensionless values and a normalized phase space equal to  $[0, 1]$ :

$$\begin{aligned}
 x_n &= \frac{V_n}{V} \in [0, 1] \quad , \quad x_{n+1} = \frac{V_{n+1}}{V} \in [0, 1] \\
 \beta &= \frac{V_U}{V} \in ]0, 1[ \quad , \quad 0 < m = \frac{V_D}{V_U} < 1 \quad , \quad \delta = e^{-\frac{T}{\tau}} \in ]0, 1[ \\
 x_b &= \frac{V_B}{V}, \quad x_a = \frac{V_A}{V}
 \end{aligned} \tag{2}$$

The following switching values in  $[0, 1]$  are:

$$\begin{aligned}
 x_a &= 1 - \frac{1-\beta}{\delta} \\
 x_b &= 1 - \frac{m(1-\beta)}{\delta}
 \end{aligned} \tag{3}$$

Finally, the circuit is modeled by the map  $x_{n+1} = F(x_n)$  (cf. Fig. 3), which is defined as follows:

$$\begin{aligned}
 \text{if } x_n \in [0, x_a[ \quad , \quad F(x_n) &= F_1(x_n) = 1 - (1 - x_n)\delta \\
 \text{if } x_n \in [x_a, x_b[ \quad , \quad F(x_n) &= F_2(x_n) = (1 - x_n)\frac{\delta\beta}{1-\beta} \\
 \text{if } x_n \in [x_b, 1] \quad , \quad F(x_n) &= F_3(x_n) = 1 - (1 - x_n)\frac{\delta}{m}\frac{1-\beta m}{1-\beta}
 \end{aligned} \tag{4}$$

It is easy to see that the map is well defined as  $F$  is continuous and maps the interval  $[0, 1]$  (the phase space of interest) into itself.

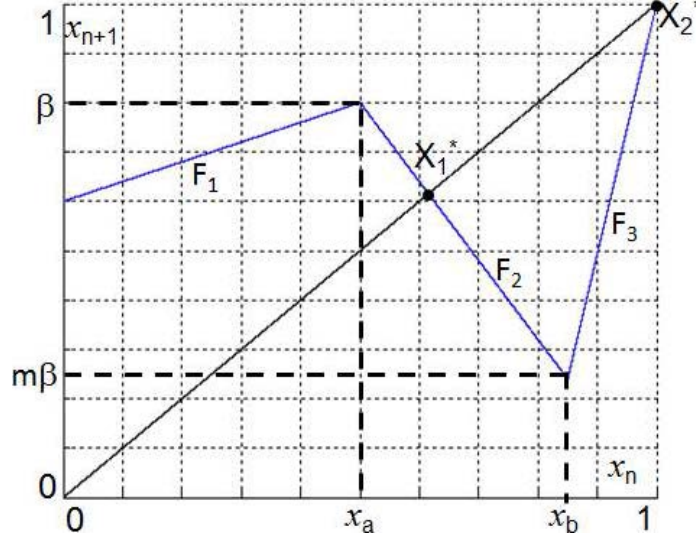


Fig. 3. The 3-pieces piecewise linear map.

## 4. Dynamical behaviour of the 1-D model

The map (4) is a 1-dimensional piecewise linear map with three pieces. In this section, we study the fixed points, order  $k$  periodic orbits and their bifurcations. We also put in evidence the homoclinic bifurcations giving rise to chaotic behaviour. First, let us give the slopes of the map, depending where is located the point in the interval  $[0, 1]$ . These values will be useful for the rest of our study.

$$\text{if } x \in [0, x_a[, \quad p_1 = \delta > 0$$

$$\text{if } x \in [x_a, x_b[, \quad p_2 = \frac{-\delta\beta}{1-\beta} < 0 \quad (5)$$

$$\text{if } x \in [x_b, 1], \quad p_3 = \frac{\delta}{m} \frac{1-\beta m}{1-\beta} > 0$$

### 4.1 Bifurcations of fixed points and order 2 periodic orbits

This study has been previously done in [4, 15]. We recall the results. Two fixed points  $X_1^*$  and  $X_2^*$  exist and are given by:

$$\begin{aligned} X_1^* &= \frac{\delta\beta}{1-\beta+\delta\beta} \in [x_a, x_b] \\ X_2^* &= 1 \end{aligned} \quad (6)$$

$X_1^*$  is stable when the slope  $p_2 = \frac{-\delta\beta}{1-\beta} \in ]-1, 0[$ , that means  $\beta < \frac{1}{1+\delta}$ .  $X_2^*$  is stable when the slope  $p_3 = \frac{\delta}{m} \frac{1-\beta m}{1-\beta} \in ]0, 1[$ , that means  $\beta < \frac{m-\delta}{m(1-\delta)}$  and  $m > \delta$ . So, we can define the bifurcation curves related to fixed points bifurcations:

$$\begin{aligned} FB1a : \beta &= \frac{1}{1+\delta}, m < \delta, \quad FB1b : \beta = \frac{1}{1+\delta}, m > \delta \\ FB1c : \beta &= \frac{m-\delta}{m(1-\delta)}, m > \delta \end{aligned} \quad (7)$$

These curves correspond to degenerate flip bifurcations,  $FB1a$  corresponds to the appearance of a stable order 2 cycle after the flip bifurcation of  $X_1^*$ ,  $FB1b$  corresponds to the appearance of an order 2 cyclic chaotic attractor  $(C_1, C_2)$ , after  $X_1^*$  has changed its stability (see Fig. 6); for instance, the order 2 periodic orbit  $(Y_1, Y_2)$ , which appears at the flip bifurcation  $FB1b$ , undergoes in the same time a border collision bifurcation ( $Y_2$  is merging with  $x_b$ ) and becomes unstable (see Fig. 5).  $FB1c$  corresponds to a border collision bifurcation for  $X_1^*$ , which disappears when merging with  $x_b$  ( $\beta$  below  $FB1b$  in the plane  $(m, \beta)$ ,  $\delta$  being fixed); at the same bifurcation value,  $X_2^*$  becomes a stable fixed point ( $\beta$  below  $FB1b$  in the plane  $(m, \beta)$ ,  $\delta$  being fixed). The curve  $FB1c$  ( $\beta$  above  $FB1b$ ) also corresponds to a degenerate bifurcation for  $X_2^*$  with the appearance of an order 2 cyclic chaotic attractor, after  $X_2^*$  has become unstable. Then, the order 2 cyclic chaotic attractor after an

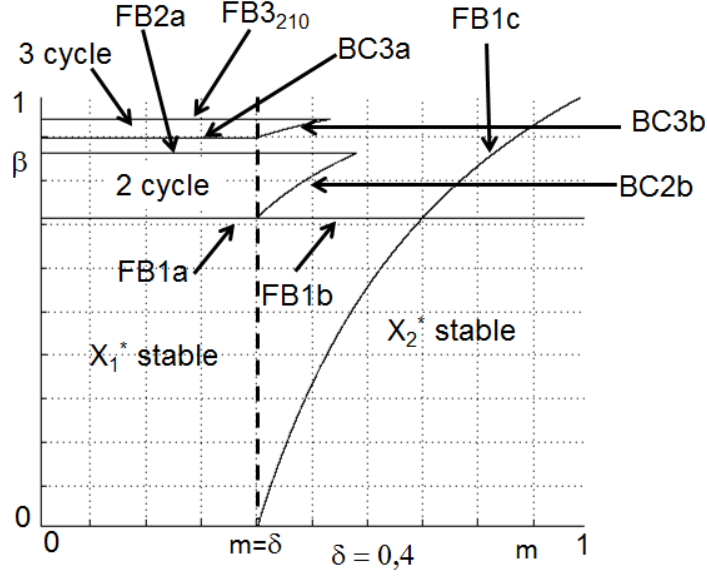


**Fig. 4.** In the  $(m, \beta)$  plane,  $\delta = 0.4$ , bifurcation curves of the map  $F$  related to fixed points and order 2 and 3 cycles.

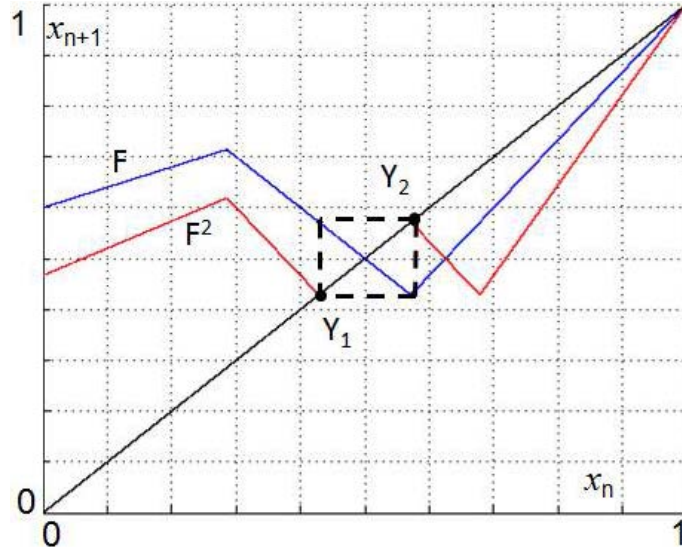


**Fig. 5.** Degenerate flip bifurcation ( $FB1b$ ) in the plane  $(x_n, x_{n+1})$  for  $\delta = 0.4$ ,  $m = 0.6$  and  $\beta = 0.7142857$ .

homoclinic bifurcation, gives rise to an one-piece chaotic attractor (see Fig. 7). Such chaos can be considered as robust in the sense of remaining chaotic even if the parameters or the initial conditions are slightly changed [1].

When there exists a stable order 2 cycle, this cycle can undergo a degenerate flip bifurcation, which gives rise to an order 4 cyclic chaotic attractor. The bifurcation curve is given by the following equation, corresponding to the slope of  $F^2$  that becomes equal to  $-1$  (see Fig. 4):

$$FB2a : \beta = \frac{1}{1+\delta^2} \quad (8)$$

$FB2a$  corresponds to the slope of  $F^2$  equal to  $p_1 p_2$  ( $F^2 = F_1 F_2$ ). It is impossible to obtain a flip bifurcation for  $F^2 = F_1 F_3$ , because  $p_1 p_3$  can never be negative.

Other bifurcation curves correspond to border collision bifurcations. It is possible to have  $F^2(x_a) = x_a$  or  $F^2(x_b) = x_b$ . The corresponding curves are respectively denoted  $BC2a$  and  $BC2b$ . Their equations are given by:

$$\begin{aligned} BC2a : \beta &= \frac{1}{1+\delta} \\ BC2b : \beta &= \frac{m-\delta^2}{m(1-\delta^2)}, m > \delta^2 \end{aligned} \quad (9)$$

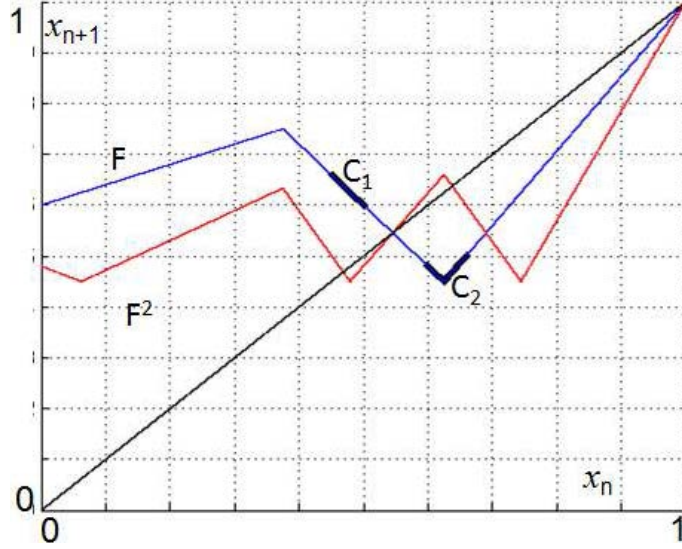


**Fig. 6.** An order 2 cyclic chaotic attractor  $(C_1, C_2)$  exists for  $\delta = 0.4$ ,  $m = 0.6$  and  $\beta = 0.75$ . Let us remark that we have plotted the chaotic attractor in the plane  $(x_n, x_{n+1})$  for a better visualization.

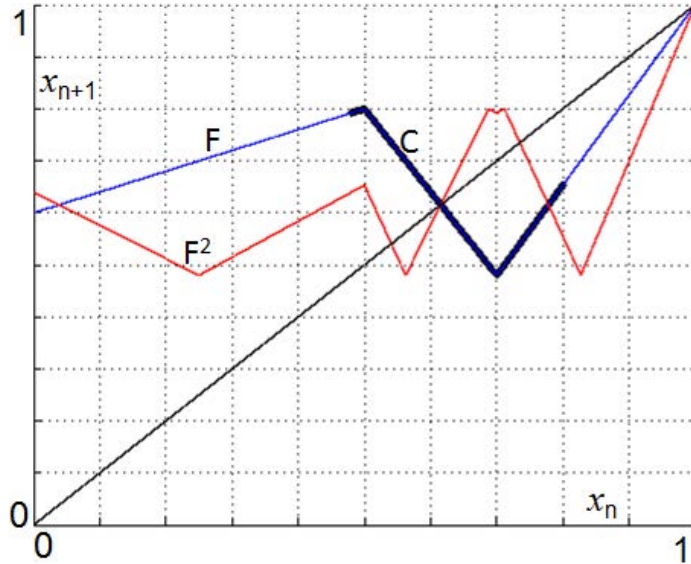


**Fig. 7.** An one-piece chaotic attractor  $C$  appears after an homoclinic bifurcation. Parameter values are  $\delta = 0.4$ ,  $m = 0.6$  and  $\beta = 0.8$ .

Let us remark that  $BC2a = FB1b$ . The bifurcation curves related to fixed points and order 2 cycles are plotted on Fig. 4.

## 4.2 Bifurcations of order $k$ periodic orbits

Using the same method as for fixed points and order 2 cycles, we can obtain the bifurcation curves for order  $k$  cycles. In this paragraph, we do not intend to study and write the bifurcation curves equations for all the categories of order  $k$  cycles that can be defined, but only for those that we have obtained in numerical simulations. Previous studies concerning bimodal piecewise linear maps have been done in a more general way [7, 12]. In this work, we only intend to give the analytical forms of bifurcation curves equations with the aim of a practical use for our model.

First, we give the bifurcation curves corresponding to the degenerate flip bifurcation. Indeed, if we consider an order  $k$  cycle, each point  $X$  of this cycle verifies  $F^k(X) = X$  and  $F^k$  is obtained by a combination of its three determinations  $F_1$ ,  $F_2$  and  $F_3$ . We can write that, in  $F^k$ ,  $F_1$  appears  $i$  times,  $F_2$   $j$  times and  $F_3$   $l$  times, with  $i + j + l = k$ . So regarding the degenerate flip bifurcation, it is

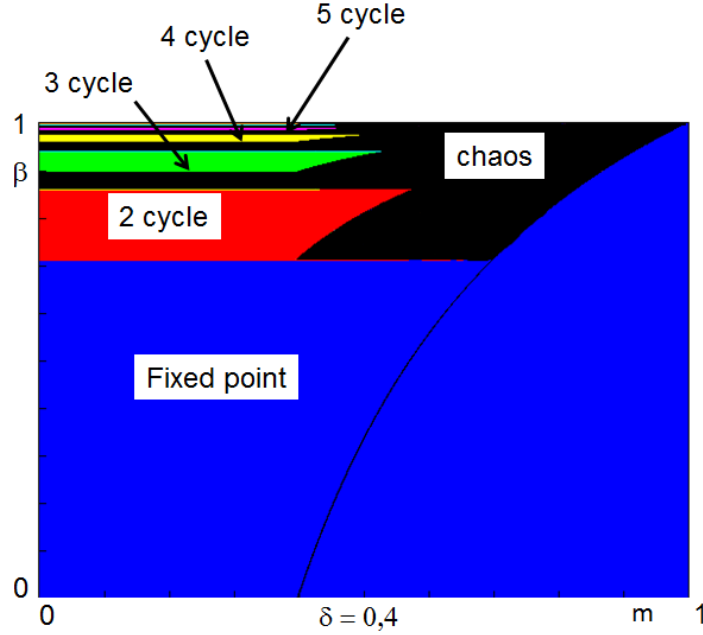


**Fig. 8.** Stability areas of  $k$  periodic orbits in the parameter plane  $(m, \beta)$  for  $\delta = 0.4$ . They are limited by bifurcation curves obtained in Fig. 4.

obtained by considering the three slopes  $p_1$ ,  $p_2$  and  $p_3$  such that  $p_1^i p_2^j p_3^l = -1$ . This curve is denoted  $FBk_{ijl}$  and is given by the following equation:

$$FBk_{ijl} : \delta^i \left(\frac{\delta\beta}{\beta-1}\right)^j \left(\frac{\delta}{m} \frac{1-\beta m}{1-\beta}\right)^l = -1, i + j + l = k, \quad (10)$$

which can also be written:

$$\delta^k = \frac{(1-\beta)^{j+l} m^l}{(1-\beta m)^l \beta^j}, i + j + l = k \quad (11)$$

All the degenerate flip bifurcation curves are known analytically and can be plotted in the parameter planes  $(\beta, \delta)$ ,  $m$  being fixed or  $(m, \delta)$ ,  $\beta$  being fixed.

It is also possible to find the border collision bifurcation curves. The collision can occur with any of both points  $x_a$  or  $x_b$ . So, we will have to look the parameter values for which one has  $F^k(x_a) = x_a$  or  $F^k(x_b) = x_b$ . Anyhow, we have to look at the way of exchanging the points of cycles by  $F$ .

The simplest case occurs when an order  $k$  cycle has its points exchanged  $k - 1$  times by  $F_1$  and one time by  $F_2$  or  $k - 1$  times by  $F_1$  and one time by  $F_3$ . It is possible to obtain the border collision bifurcation curves, which are denoted  $BCka$  if the collision occurs with  $x_a$ , that means  $F^k(x_a) = x_a$ , or  $BCkb$  if the collision occurs with  $x_b$ , that means  $F^k(x_b) = x_b$ . The corresponding equations are:

$$\begin{aligned} BCka : \beta &= \frac{1-\delta^{k-1}}{1-\delta^k}, m < \delta \\ BCkb : \beta &= \frac{m-\delta^2}{m(1-\delta^2)}, m > \delta^2 \end{aligned} \quad (12)$$

On Fig. 4 are plotted the bifurcation curves of an order 3 cycle whose exchange of points is given by  $F_1^2 F_2$ . Figure 8 gives the areas of stability of order  $k$  periodic orbits,  $k = 1, \dots, 5$ , it is very easy to observe that these areas are limited by the bifurcation curves obtained in Fig. 4. An enlargement of these figures is provided in Fig. 9 and Fig. 10, which permits to put in evidence order 6 and 7 cycles. Bifurcation curves of order  $k$  cycles,  $k = 1, \dots, 7$  are plotted on Fig. 10. All these cycles are cycles of  $F^k = F_1^{k-1} F_2$ . Let us remark that we obtain a period-adding sequences of periodic orbits. Between two stability areas of periodic orbits, chaos appears ( $k$ -pieces chaotic attractor), which undergoes a succession of homoclinic bifurcations giving rise to an one-piece chaotic attractor.

On Fig. 8, we consider the parameter plane  $(\delta, \beta)$ ,  $m$  being fixed and equal to 0.4, we can see the stability areas of some order  $k$  cycles,  $k = 1, \dots, 5$ . On Fig. 12 and Fig. 13, an enlargement permits to obtain order  $k$  cycles,  $k = 1, \dots, 7$ . Those cycles have their points exchanged as given below (we consider the cycles from left to right in the figures). It is also possible to use *Symbolic Dynamics* of a

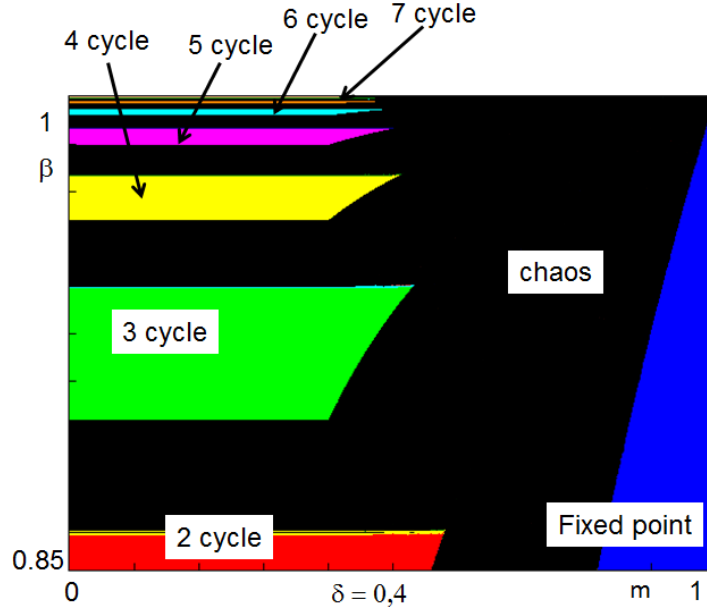


Fig. 9. Enlargement of Fig. 8, order  $k$  cycles are observed,  $k = 1, \dots, 7$ .

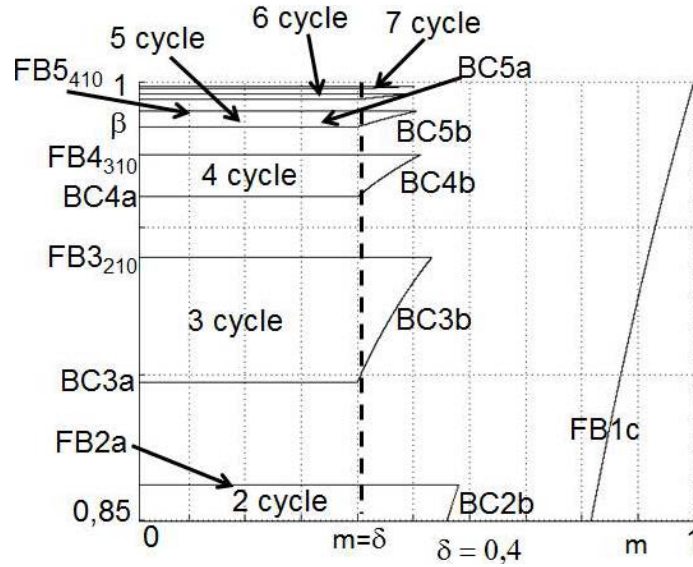
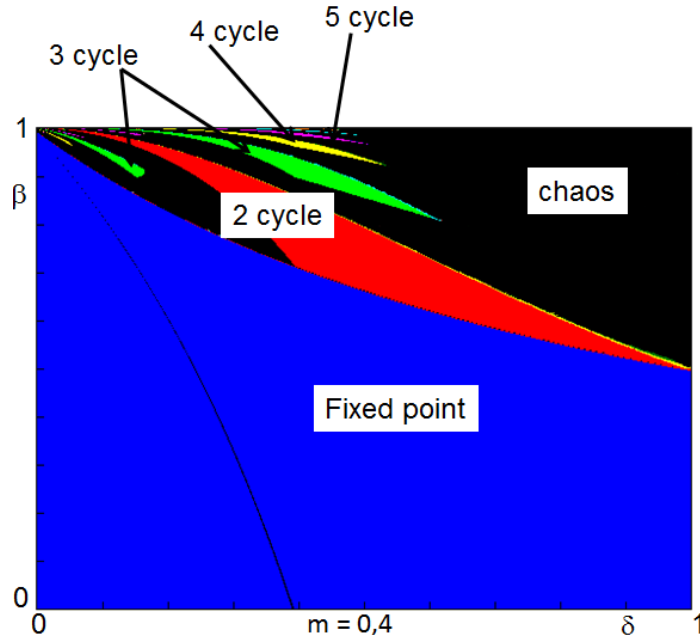


Fig. 10. Bifurcation curves corresponding to the limit of stability regions of Fig. 9 in the parameter plane  $(m, \beta)$  for  $\delta = 0.4$ .

bimodal map [13, 14], we have chosen to represent a cycle by beginning with the point at the left of the interval  $[0, 1]$  (generally, this point is located inside  $I_1$  and  $F_1$  is applying). The use of symbolic dynamics corresponds to give a code to every order  $k$  cycle by considering the location of the points in the intervals  $I_1, I_2$  or  $I_3$ ; generally, the following rule is used: a point of the cycle is coded by  $L$  when it belongs to  $I_1$ ,  $M$  when it belongs to  $I_2$  and  $R$  when it belongs to  $I_3$  (sometimes, the codes  $A$  or  $B$  can be used if one point of the cycle is merging with  $x_a$  or  $x_b$ , in this paper, we will not take this possibility into account). Here are the obtained coding for the cycles of Fig. 12 from left to right in the figure:

- order 6 cycle,  $F_2 F_3^4 F_1, LRRRRM$
- order 5 cycle,  $F_2 F_3^3 F_1, LRRRM$
- order 4 cycle,  $F_2 F_3^2 F_1, LRRM$
- order 7 cycle,  $F_2 (F_3^2 F_1)^2, LRRLRRM$



**Fig. 11.** Stability areas of  $k$  periodic orbits,  $k = 1, 2, 3$  in the parameter plane  $(\delta, \beta)$  for  $m = 0.4$ .

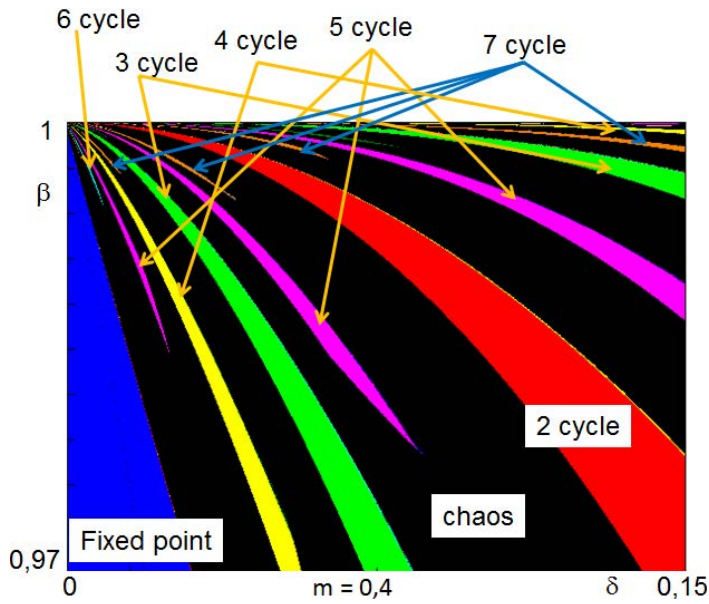


**Fig. 12.** Enlargement of Fig. 11. Stability areas of  $k$  periodic orbits,  $k = 1, \dots, 7$  in the parameter plane  $(\delta, \beta)$  for  $m = 0.4$ . They are limited by bifurcation curves obtained in Fig. 13.

- order 3 cycle,  $F_2F_3F_1$ ,  $LRM$
- order 5 cycle,  $F_2(F_3F_1)^2$ ,  $LRLRM$
- order 7 cycle,  $F_2(F_3F_1)^3$ ,  $LRLRLRM$
- order 2 cycle,  $F_2F_1$ ,  $LM$
- order 7 cycle,  $F_1F_2F_1(F_3F_1)^2$ ,  $LRLRLML$
- order 5 cycle,  $F_1F_2F_1F_3F_1$ ,  $LRLML$
- order 3 cycle,  $F_2F_1^2$ ,  $LLM$

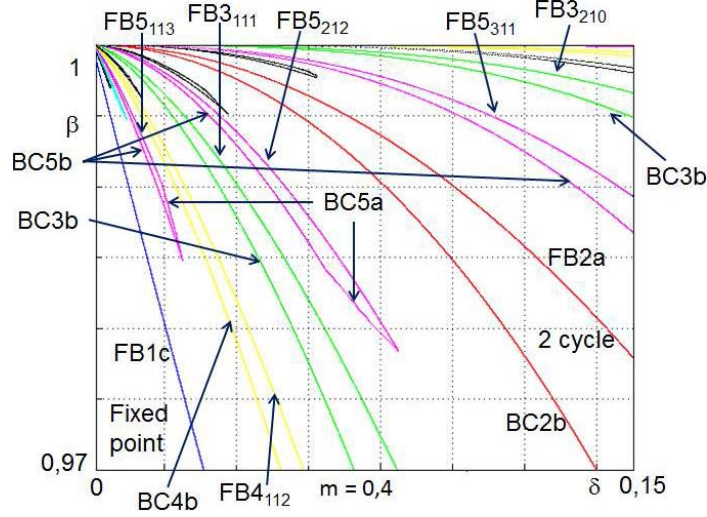


**Fig. 13.** Bifurcation curves of  $k$  periodic orbits,  $k = 1, 2, 3, 4, 5, 6, 7$  in the parameter plane  $(\delta, \beta)$  for  $m = 0.4$ . They limit the stability areas of Fig. 12. In order to clarify the figure, only bifurcation curves for  $k = 1, \dots, 5$  have been indicated.

- order 7 cycle,  $F_2F_1^2F_3F_1^3$ ,  $LLLRLLM$
- order 4 cycle,  $F_2F_1^3$ ,  $LLM$

All the stability areas in Fig. 12 are bounded by degenerate flip bifurcation curves  $DFBk_{ijl}$  (10) or border collision bifurcation curves. The border collision bifurcation curves must be calculated by considering the exchange of the points of the cycle and the point  $x_a$  or  $x_b$  with which there is a collision. The cycles above can be classified in different categories, related to the kind of symbols which represent them or regarding the way of exchanging their points. We can propose the following classification and give the equations of the border collision bifurcation curves for each of them (let us recall that the degenerate flip bifurcation curves are given by (10)(11)):

- The order 2 cycle ( $F_2F_1$ ,  $LM$ ), the order 3 cycle ( $F_2F_1^2$ ,  $LLM$ ) and the order 4 cycle ( $F_2F_1^3$ ,  $LLM$ ) have already been studied and their bifurcation curves are given in (10)(11)(12).
- The order 6 cycle ( $F_2F_3^4F_1$ ,  $LRRRRM$ ), the order 5 cycle ( $F_2F_3^3F_1$ ,  $LRRRM$ ), the order 4 cycle ( $F_2F_3^2F_1$ ,  $LRRM$ ) and the order 3 cycle ( $F_2F_3F_1$ ,  $LRM$ ) belong to the same class of order  $k$  cycle, which can be denoted:  $F_2F_3^{k-2}F_1$ ,  $LR\dots RM$ , where the symbol  $R$  appears  $(k-2)$  times. The border collision bifurcation curves are given by:

$$\begin{aligned} BCka : \frac{\delta^k(1-\beta m)^{k-2}\beta + (1-\beta)^{k-1}m^{k-2}}{\delta(1-\beta)^{k-2}m^{k-2}} &= 1, \\ BCkb : \delta^k &= \left(\frac{1-\beta}{1-\beta m}\right)^{k-1} \end{aligned} \quad (13)$$

- The order 5 cycle ( $F_2(F_3F_1)^2$ ,  $LRLRM$ ) and the order 7 cycle ( $F_2(F_3F_1)^3$ ,  $LRLRLRM$ ) belong to the same category of order  $k$  cycle,  $k$  odd, which can be denoted:  $F_2(F_3F_1)^{\frac{k-1}{2}}$ ,  $LRLR\dots M$ , where the symbol  $LR$  appears  $\left(\frac{k-1}{2}\right)$  times. The border collision bifurcation curves are given by:

$$\begin{aligned} BCka : \frac{\delta^{k-2}(1-\beta m)^{\frac{k-3}{2}}}{m^{k-4}(1-\beta)^{\frac{k-1}{2}}} - \frac{\delta^k\beta(1-\beta m)^{\frac{k-1}{2}}}{m^{k-3}(1-\beta)^{\frac{k+1}{2}}} &= 1, \\ BCkb : \delta^k &= \left(\frac{1-\beta}{1-\beta m}\right)^{\frac{k+1}{2}} \end{aligned} \quad (14)$$

- Concerning the order 7 cycle ( $F_2(F_3^2F_1)^2$ ,  $LRRLRRM$ ), we only give its own bifurcation curves:

$$\begin{aligned} BCka : -\frac{\delta^7\beta(1-\beta m)^4}{m^4(1-\beta)^5} + \frac{\delta^4(1-\beta m)^2}{m^2(1-\beta)^3} &= 1, \\ BCkb : \delta^7 &= \left(\frac{1-\beta}{1-\beta m}\right)^5 \end{aligned} \quad (15)$$

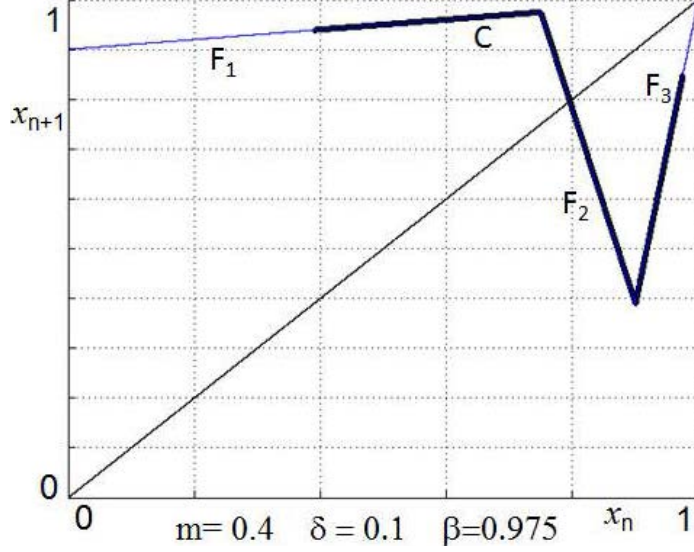


**Fig. 14.** A chaotic attractor is located in the three intervals  $I_1$ ,  $I_2$  and  $I_3$  and is issued from an order 3-cycle whose points are exchanging using the three determinations of  $F$ .

- The order 7 cycle  $(F_1F_2F_1(F_3F_1)^2, LRLRLML)$  and the order 5 cycle  $(F_1F_2F_1F_3F_1, LRLML)$  belong to the same category of order  $k$  cycle,  $k$  odd, which can be written under the following general form:  $F_1F_2F_1(F_3F_1)^{\frac{(k-2)}{3}}, LRLR\dots LRLML$ , where the symbol  $LR$  appears  $\frac{k-3}{2}$  times. The border collision bifurcation curves are given by:

$$\begin{aligned} BCka : \frac{\delta^2}{(1-\beta)} - \frac{\delta^k \beta (1-\beta m)^{\frac{k-3}{2}}}{m^{\frac{k-3}{2}} (1-\beta)^{\frac{k-1}{2}}} &= 1, \\ BCkb : \delta^k &= \left( \frac{(1-\beta)m}{(1-\beta m)} \right)^{k-3} \end{aligned} \quad (16)$$

- Concerning the order 7 cycle  $(F_2F_1^2F_3F_1^3, LLLRLLM)$ , we only give its own bifurcation curves:

$$\begin{aligned} BCka : \frac{\delta^3}{(1-\beta)} - \frac{\delta^7 \beta (1-\beta m)}{m(1-\beta)^2} &= 1, \\ BCkb : \delta^7 &= \left( \frac{(1-\beta)m}{(1-\beta m)} \right)^2 \end{aligned} \quad (17)$$

All the bifurcation curves for order  $k$  cycles,  $k = 1, \dots, 7$  are plotted on Fig. 13. They clearly limit the stability areas of order  $k$  cycles of Fig. 12. The curves of degenerate flip bifurcations and border collision with  $x_b$  are given in an explicit form and can be directly plotted, the curves related to the border collision with  $x_a$  are given under an implicit form and have to be plotted by using a numerical method (Newton-Raphson).

Between two stability regions, there exists a chaotic attractor. The chaotic attractor issued from a degenerate flip bifurcation is a cyclic one, then after a succession of homoclinic bifurcations, it becomes an one-piece chaotic one.

For some parameter values, chaos can be located on the three domains  $I_1$ ,  $I_2$  and  $I_3$  (Fig. 14). This chaos is obtained from border collision bifurcations of order  $k$ -cycles whose points exchange by  $F_1$ ,  $F_2$  and  $F_3$ . This is the case around the stability area of the order 3-cycle  $(F_2F_3F_1, LRM)$ (see Fig. 12). In this case, chaos can be considered as robust; indeed its existence domain in the parameter space is large enough.

## 5. Conclusions

We have proposed a very simple circuit under the form of a hybrid system, which presents two major interests. First, this circuit is modeled by a one-dimensional piecewise bimodal linear map, such map exhibits very rich signals properties and dynamics. Secondly, such a circuit allows to produce chaotic signals, which can be robust in the sense of remaining chaotic even if the parameters or the initial conditions are slightly changed; such chaotic signals can be very useful for different kinds of

applications. The model is very simple and depends on three parameters, we have been able to derive the exact analytical expressions of degenerate flip bifurcation and border collision bifurcation curves in the parameter space for some periodic orbits. The border collision bifurcations give rise to chaos, which can be robust, depending upon parameter values and configurations of periodic orbit sequences in parameter space. We intend to continue our study, in order to have a more general classification of all periodic orbits of the map. This will help to have a good understanding of the dynamical behaviour of the circuit and, depending on the intended application, to propose suitable sets of parameters values.

## Acknowledgments

We thank Professor Laura Gardini for interesting and helpful discussions and advices.

## References

- [1] S. Banerjee, J.A. Yorke, and C. Grebogi, "Robust chaos," *Physical Review Letters*, 80, pp. 3049–3052, 1998.
- [2] S. Banerjee, P. Ranjan, and C. Grebogi, "Bifurcations in 2D piecewise smooth maps - theory and applications in switching circuits," *IEEE Trans. Circuits Systems I*, vol. 47, pp. 633–643, 2000.
- [3] S. Mandal and S. Banerjee, "An integrated CMOS chaos generator," *National Conference on Nonlinear and Dynamics*, Indian Institute of Technology, December 2003.
- [4] D. Fournier-Prunaret, P. Chargé, and L. Gardini, "Border collision bifurcations and chaotic sets in a two-dimensional piecewise linear map," *Communications in Nonlinear Science and Numerical Simulations*, vol. 16, no. 2, pp. 916–927, 2011.
- [5] L. Gardini, D. Fournier-Prunaret, and P. Chargé, "Border collision bifurcations in a two-dimensional PWS map from a simple circuit," *Chaos* 21, 023106 (2011), doi:10.1063/1.3555834.
- [6] T. Kousaka, T. Kido, T. Ueta, H. Kawakami, and M. Abe, "Analysis of Border-Collision Bifurcation in a Simple Circuit," *IEEE International Symposium on Circuits and Systems (ISCAS'00)*, Geneva, Switzerland, May 2000.
- [7] A. Panchuk, "Three segmented piecewise linear map," *International Workshop on Nonlinear Maps and Applications (NOMA'11)*, Evora, Portugal, September 15-16, 2011.
- [8] T. Kousaka, Y. Yasuhara, T. Ueta, and H. Kawakami, "Experimental realization of controlling chaos in the periodically switched nonlinear circuit," *Int. J. Bifurcation and Chaos*, vol. 14, no. 10, pp. 3655–3660, 2004.
- [9] I. Sushko and L. Gardini, "Degenerate bifurcations and border collisions in piecewise smooth 1D and 2D maps," *Int. J. Bifurcation and Chaos*, vol. 20, no. 7, pp. 2045–2070, 2010.
- [10] P. Chargé, D. Fournier-Prunaret, and L. Gardini, "Two-dimensional piecewise defined maps realized with a simple switching circuit," *International Conference on Nonlinear Theory and Applications (NOLTA'08)*, Budapest, Hungary, September 2008.
- [11] D. Fournier-Prunaret and P. Chargé, "Bifurcation structure in a circuit modeled by a 1-dimensional piecewise linear map," *IEICE International Conference on NonLinear Theory and Applications (NOLTA'11)*, Kobe, Japan, September 2011.
- [12] Yu.L. Maistrenko, V.L. Maistrenko, and S.I. Vikul, "On period-adding sequences of attracting cycles in piecewise linear maps," *Chaos, Solitons and fractals*, vol. 9, no. 1/2, pp. 67–75, 1998.
- [13] J.P. Lampreia and J. Sousa Ramos, "Symbolic dynamics of bimodal maps," *Portugaliae Mathematica*, vol. 54, no. 1, pp. 1–18, 1997.
- [14] N. Martins, R. Severino, and J. Sousa Ramos, "Isentropic real cubic maps," *Int. J. of Bifurcation and Chaos in Applied Sciences and Engineering*, vol. 13, no. 7, pp. 1701–1709, 2003.
- [15] D. Fournier-Prunaret, P. Chargé, and L. Gardini, "Chaos generation from 1D or 2D circuits including switches," *IEEE International Conference for Internet Technology and Secured Transactions (ICITST)*, Dubai, UAE, December 12-13, pp.86–90, 2011.